IEEE Access
Multidisciplinary | Rapid Review | Open Access Journal

SPECIAL SECTION ON NEW WAVEFORM DESIGN AND AIR-INTERFACE FOR FUTURE HETEROGENEOUS NETWORK TOWARDS 5G

Received February 2, 2018, accepted March 4, 2018, date of publication March 12, 2018, date of current version April 4, 2018.

Digital Object Identifier 10.1109/ACCESS.2018.2814682

Pseudo-Noise Sequence Based Synchronization for Generalized Frequency Division Multiplexing in 5G Communication System

ZHENYU NA[1],(Member, IEEE), MENGSHU ZHANG[1], MUDI XIONG[1], JUNJUAN XIA[2], XIN LIU[3],(Member, IEEE), AND WEIDANG LU[4], (Member, IEEE)

[1]School of Information Science and Technology, Dalian Maritime University, Dalian 116026, China
[2]School of Computer Science and Educational Software, Guangzhou University, Guangzhou 510006, China
[3]School of Information and Communication Engineering, Dalian University of Technology, Dalian 116024, China
[4]College of Information Engineering, Zhejiang University of Technology, Hangzhou 310023, China

Corresponding authors: Zhenyu Na (nazhenyu@dlmu.edu.cn) and Xin Liu (liuxinstar1984@dlut.edu.cn)

This work was supported in part by the National Natural Science Foundations of China under Grant 61301131 and Grant 61601221, in part by the Natural Science Foundations of Jiangsu Province under Grant BK20140828, in part by the China Postdoctoral Science Foundations under Grant 2015M580425, and in part by the Fundamental Research Funds for the Central Universities under Grant 3132016347 and Grant DUT16RC(3)045.

ABSTRACT As one of the candidate waveforms for 5G, generalized frequency division multiplexing (GFDM) is a flexible non-orthogonal multicarrier technique. Similar to orthogonal frequency division multiplexing, GFDM communication system suffers from symbol timing offset (STO) and carrier frequency offset (CFO) caused by multipath effect and Doppler shift. In this paper, we design a pseudo noise (PN) based preamble and propose an approach for signal synchronization. The preamble is composed of two identical PN sequences whose autocorrelation and cross-correlation are better than cyclic prefix (CP). STO can be detected by calculating the correlation coefficient between the local PN sequence of receiver and the corresponding preamble part of sliding window. These two adjacent PN sequences can be used to calculate phase offset value by Fourier transform, and then obtain CFO value. Simulation results demonstrate that, compared with conventional CP-based synchronization, the proposed approach has the lower mean square error and symbol error rate at the cost of just a little bit more bandwidth.

INDEX TERMS 5G, GFDM, non-orthogonal multicarrier, synchronization, OFDM.

I. INTRODUCTION

In the fourth generation (4G) mobile communications, Orthogonal Frequency Division Multiplexing (OFDM) is widely used as the core technology of physical layer [1] because of its high spectrum utilization, strong capability to combat interference and fading. However, the physical layer of the fifth generation (5G) mobile communications puts forward higher demands on flexibility, reliability, spectral efficiency, robustness and scalability. For example, the tactile Internet requires extremely low latency; the Enhanced Broadband needs a transmission rate up to 10Gbps; Low-power Machine-Type Communications (MTC) need to support massive connectivity [2]; Wireless Regional Area Network (WRAN) requires greater coverage. In this context, OFDM cannot adapt to different applications and scenarios in 5G communication system. Therefore, OFDM is not the best waveform for future 5G physical layer [3]. Both Filter Bank Multi-Carrier (FBMC) and Generalized Frequency Division Multiplexing (GFDM) are candidate waveforms for 5G [4]. Since they do not require orthogonality, power loss can be reduced. Also, their Out-of-Band (OOB) leakage can be reduced by non-rectangular pulse shaping. Since FBMC uses filter bank for modulation and demodulation, it does not require strict synchronization between subcarriers. However, the design of prototype filter has to meet the specific requirements of frequency response, which leads to the high complexity of system implementation [5]. In contrast, GFDM is a flexible waveform, whose data block has a two-dimensional structure in time and frequency domain. Compared with FBMC, GFDM has the lower equalization complexity at receiver and is more suitable for burst signal transmission. Therefore, GFDM is more competitive and advantageous

in 5G communications. Therefore, we choose GFDM as the waveform to be studied in this paper.

Multipath effect and Doppler shift in wireless communications would lead to Symbol Timing Offset (STO) and Carrier Frequency Offset (CFO), which have great impacts on the reliability and effectiveness of signal transmission. Therefore, good synchronization approaches are necessary to reduce the error caused by STO and CFO. For OFDM communication system, there are many solutions to synchronization problems. A reduced-complexity maximum likelihood estimation synchronization approach based on Cyclic Prefix (CP) was proposed in [6]. A symbol timing synchronizer for OFDM system based on Pseudo-Noise (PN) sequence was proposed in [7]. A training sequence based timing synchronization approach for Power Line Communication (PLC) was proposed in [8] for OFDM systems.

Though there are many similarities between GFDM and OFDM, their data block structures are quite different. It leads to that the synchronization approaches used in OFDM cannot be applied to GFDM directly. Therefore, the synchronization for GFDM system is an urgent problem to be solved. There are still few research results of GFDM synchronization. An analytic model that evaluates Bit Error Rate (BER) performance of GFDM in the case of imperfect synchronization was proposed in [9]. The impacts of STO and CFO on GFDM system were analyzed in [10] where the Signal-to-Interference Ratio (SIR) performance between GFDM and OFDM systems in the presence of STO and CFO was compared. A synchronization approach based on embedded training sequences in the payload of GFDM symbol was proposed in [11]. A CP-based synchronization approach was proposed in [12] which utilizes the side-lobe of prototype filter to achieve data repeatability. However, the expansion of estimation range has to rely on large amounts of data.

As analyzed above, CP-based synchronization is a common approach. Due to the particularity of GFDM data block structure, the direct application of CP-based synchronization to GFDM system is restricted. To cope with the limitation, a PN sequence based synchronization approach is proposed in this paper. The main contributions of the paper are summarized as follows:

- We design a novel preamble consisting of two identical PN sequences. Unlike the conventional single PN sequence based preamble, STO and CFO can be detected only inside the preamble to achieve higher detection accuracy without involving GFDM data part.
- We improve the accuracy of STO detection by using the proposed preamble because of its good autocorrelation and cross-correlation. We use a sliding window and make it slide point by point. By calculating the correlation coefficient between the local PN sequence of receiver and the corresponding part of the window, the STO value can be obtained by the peak of correlation coefficient.
- We deal with phase flip and expand CFO detection range. We use Fourier transform to simplify the calculation of phase difference between the two PN sequences and obtain CFO value. Since the two PN sequences are contiguous, the possible phase flip caused by successive GFDM sub-symbols can be eliminated. Thus, the detection range is expanded.

The remaining of the paper is organized as follows. In Section 2, the synchronization model of GFDM communication system and the impacts of STO and CFO on the system are expounded. In Section 3, the traditional CP-based synchronization is analyzed. In Section 4, a PN sequence based synchronization is proposed whose advantages over the traditional approach are analyzed. In Section 5, the two approaches described in Section 3 and Section 4 are simulated, compared and discussed. Section 6 concludes this paper.

II. SYNCHRONIZATION MODEL FOR GFDM COMMUNICATION SYSTEM

The GFDM communication system model is shown in Fig. 1. The data source $\boldsymbol{b}$ is a binary data stream. After encoding, reshaping and mapping operations, a $K \times M$ matrix $\vec{d} = (\vec{d}_0^T, \vec{d}_1^T, \ldots, \vec{d}_m^T, \ldots, \vec{d}_{M-1}^T)$ is formed, where $\vec{d}_m = (d_{0,m}, d_{1,m}, \ldots, d_{k,m}, \ldots, d_{K-1,m})$. Specifically, GFDM data block contains M sub-symbols and each sub-symbol has K subcarriers. $g_{k,m}$ is the pulse shaping function corresponding to the element $d_{k,m}$. After pulse shaping, the transmit symbol is given by

$$x[n] = \sum_{k=0}^{K-1} \sum_{m=0}^{M-1} g_{k,m}[n] d_{k,m}, \quad n = 0, 1, \cdots, N-1, \quad (1)$$

(1) can be expressed by its vector form as below

$$\vec{x} = \boldsymbol{A}\vec{d}, \quad (2)$$

Where $\boldsymbol{A}$ is a $KM \times KM$ transmission matrix whose expression is given by

$$\boldsymbol{A} = (\vec{g}_{0,0}, \cdots, \vec{g}_{K-1,0}, \vec{g}_{0,1}, \cdots, \vec{g}_{K-1,M-1}). \quad (3)$$

After pulse shaping and CP adding operations, the signal $\vec{x}$ is windowed. Followed by parallel-serial conversion, the signal $\vec{x}$ with CP is sent to channel and transmitted to the receiver. The received signal $\vec{x}_{ch}$ is given by

$$\vec{x}_{ch} = \boldsymbol{H}\vec{x} + \boldsymbol{N}, \quad (4)$$

Where $\boldsymbol{H}$ is the channel matrix; $\boldsymbol{N}$ is the noise matrix.

The received signal needs to be synchronized to correct the error caused by STO and CFO. After the synchronized signal is demodulated, demapped and decoded, a data stream with low Bit Error Rate (BER) can be obtained, and then the receiver can recover the original information. In the following sections, two different synchronization approaches will be analyzed in detail.

In fact, the received signal (4) would suffer from STO and CFO. Multipath effect is one of the main causes of STO [11]. The STO in different situations is shown in Fig. 2.

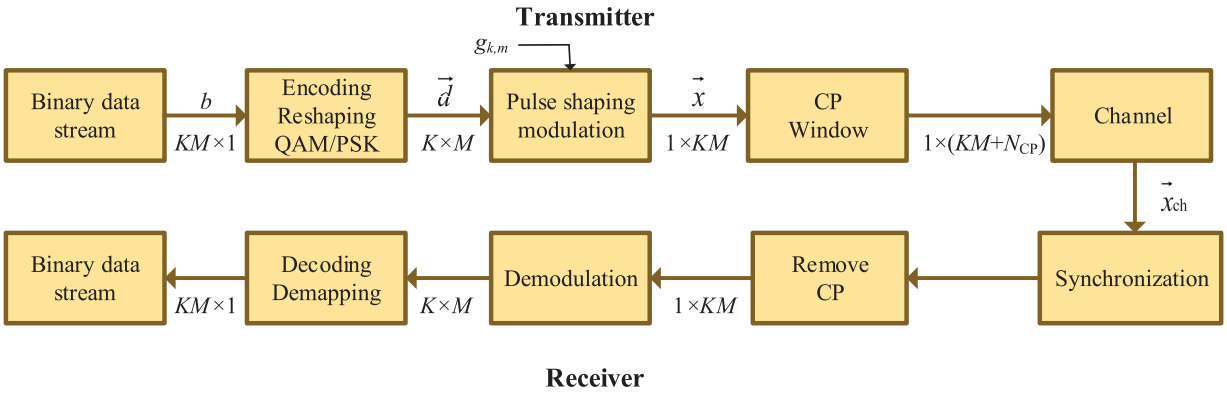

FIGURE 1. GFDM communication system model.

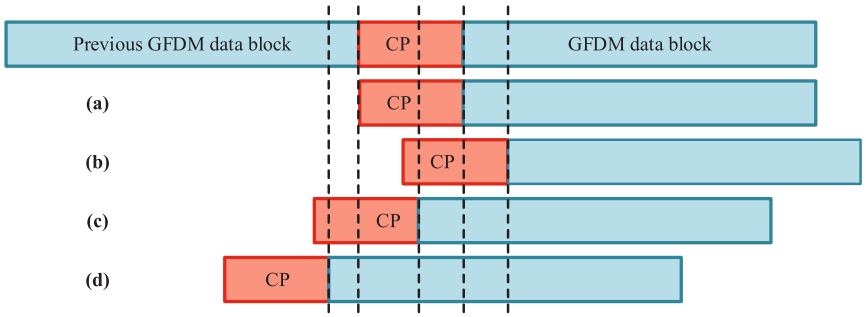

FIGURE 2. STO in different situations.

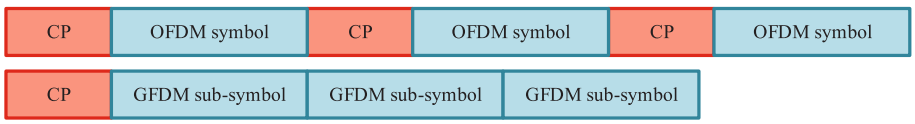

FIGURE 3. Structural difference between OFDM and GFDM symbol.

In Fig. 2, case (a) shows the perfect synchronization. Case (b) shows that the estimation point lags behind the standard point. Specifically, the overlap between successive GFDM data blocks would happen that leads to Inter-Symbol Interference (ISI). Case (c) and (d) indicate that the estimation point is ahead of the standard point. For case (c), since STO is less than the length of CP, the current GFDM data block is not subject to the impact of the previous one. For case (d), since STO is larger than the length of CP, the successive GFDM data blocks overlap with each other resulting in ISI and Inter-Carrier Interference (ICI).

Fig. 3 demonstrates the structural difference between OFDM and GFDM symbol. Different from OFDM, GFDM data block has a two-dimensional structure consisting of multiple sub-symbols. When synchronization is lost, the entire GFDM data block suffers from STO resulting in higher error rate. In this section, the impact of STO on the SER in GFDM system is simulated when STO values are 0, ±1 and ±10 samples, respectively. Simulation results are shown in Fig. 4.

It can be seen from Fig. 4 that STO affects SER performance distinctly. As long as STO value is not equal to 0, SER reaches about 0.9 and almost keeps unchanged. However, the synchronization efficiency of GFDM system is higher than OFDM system because of the following reason. One GFDM data block contains multiple sub-symbols, while one OFDM data block includes only one sub-symbol. In the case of the same number of sub-symbols, OFDM system needs to detect the offset of each sub-symbol separately, while GFDM system synchronizes multiple sub-symbols simultaneously.

Doppler shift and the mismatch between local oscillators at the transmitter and receiver are the major causes of CFO. In this section, the impact of CFO on the SER in GFDM system is simulated when the normalized CFO values are 0, 0.01, 0.03, 0.05 and 0.1, respectively. Simulation results are shown in Fig. 5.

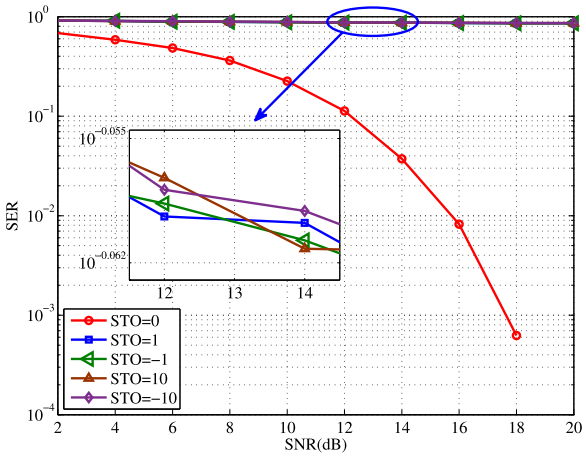

FIGURE 4. Impact of STO on SER for GFDM system.

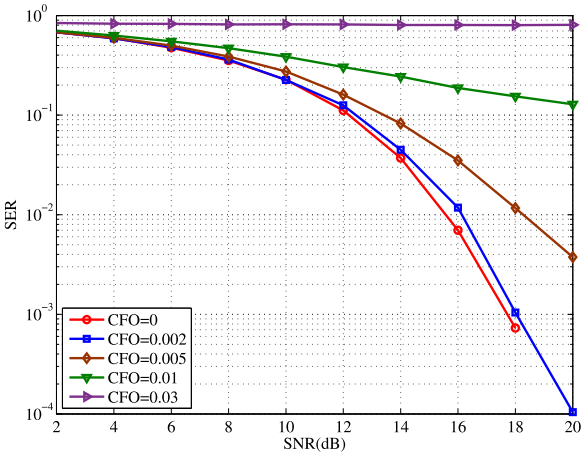

FIGURE 5. Impact of CFO on SER for GFDM system.

In contrast to the impact of STO, the different values of CFO correspond to the different curves of SER. As shown in Fig. 5, for a fixed SNR, SER increases with the increase of CFO value. The existence of CFO leads to the generation of phase offset and deteriorates SER performance. As CFO increases, the phase offset becomes larger. When CFO exceeds a certain value, in other words, the resulting phase offset exceeds π, a phase flip is produced and the system SER is greatly deteriorated.

III. CP-BASED SYNCHRONIZATION

Since the loss of synchronization has a great impact on the system reliability, a good synchronization approach is necessary. As the non-data-assisted approach, CP-based synchronization is traditionally used in OFDM system. Without adding additional assistance data, it requires only data itself and has the higher efficiency than the data-assisted synchronization approaches. The CP-based synchronization model is shown in Fig. 6.

The length of CP is denoted by N_{CP}. The double sliding windows w_1 and w_2 whose length is N_{CP} slide point by point from front to back. The length of GFDM data is equal to the distance between w_1 and w_2. The cross-correlation coefficient of the corresponding data parts of w_1 and w_2 is calculated as

$$R_{CP}(n) = \sum_{i=n}^{n+K-1} r(i) \times r(i+N), \tag{5}$$

Where $N = K \times M$, r represents the data parts of w_1 and w_2. In this case, the STO detection result n_{CP} can be obtained by detecting the peak of R_{CP} which is expressed as

$$n_{CP} = \text{argmax}\, R_{CP}(n), \tag{6}$$

When $n_{CP} = 0$, the double sliding windows are exactly at the standard point that means perfect synchronization. When $n_{CP} < 0$, the data is ahead of the standard point. When $n_{CP} > 0$, the data lags behind the standard point.

Fig. 7 shows the correlation coefficient curve of CP-based synchronization. With a CP length of 128 samples, the sliding distance of the double sliding windows is 256 samples. Since CP is copied from a part of GFDM data block, the judgement accuracy based on the correlation coefficient between w_1 and w_2 is low. For example, when *STO*=10, as demonstrated in Fig. 7, it can be seen that the correlation coefficient in the proximity of the actual offset position (n = 118) is similar. As a result, the misjudgment would happen and lead to errors.

In CFO synchronization, the CFO of w_2 is M times than w_1 because of M sub-symbols contained in GFDM data block. The following expression holds

$$W_2(k) = W_1(k)e^{j2\pi M\varepsilon}, \tag{7}$$

Where W_1 and W_2 can be obtained after w_1 and w_2 are transformed by using Fast Fourier Transform (FFT), respectively. $2\pi M\varepsilon$ is the phase offset value. In the actual detection, only the normalized ε needs to be detected to obtain the estimated CFO value.

According to (7), the CFO detection range of CP-based synchronization is $(-\pi/M, \pi/M)$. After passing channel, a phase flip occurs if the actual CFO is larger than π/M or smaller than $-\pi/M$. It would make synchronization more difficult. Therefore, it is necessary to determine whether a phase flip does happen. Once a phase flip is detected, it should be corrected before synchronization.

In summary, CP-based synchronization has the disadvantages of insignificant correlation peak and possible phase flip. To overcome these limitations, a PN sequence based synchronization is proposed in the next section.

IV. PN SEQUENCE BASED SYNCHRONIZATION

PN sequence is a commonly-used preamble sequence whose advantages lie in its good autocorrelation and cross-correlation. There are several types of PN sequences, such as shift register sequence, Gold sequence and GMW sequence. As a type of shift register sequences, the m sequence has the lower generation complexity compared with the M sequence. Therefore, the m sequence is selected as the PN sequence in this section. The synchronization model based on PN sequence is shown in Fig. 8.

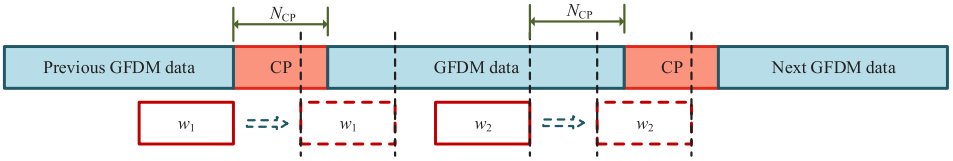

FIGURE 6. CP-based synchronization model.

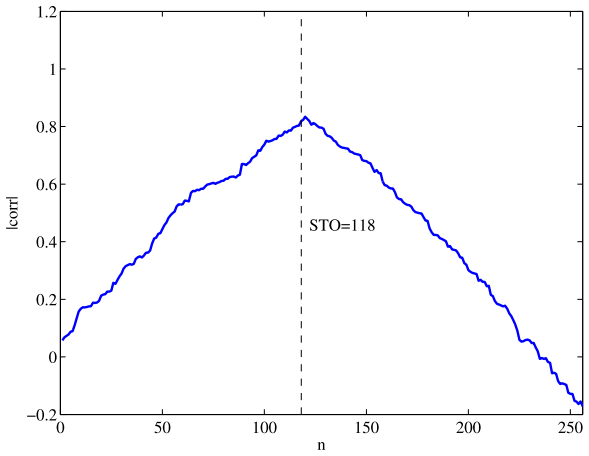

FIGURE 7. Correlation coefficient curve of CP-based synchronization.

The preamble sequence in Fig. 8 contains two identical PN sequences y_1 and y_2 with the same length of K. After encoding, reshaping, mapping, and pulse shaping operations, the modulated PN sequence x_{PN} is derived as

$$x_{PN} = \boldsymbol{A}_{PN}\boldsymbol{d}_{PN}, \tag{8}$$

Here, x_{PN} can still be windowed to reduce the OOB leakage. Then, the modulated PN sequence is transmitted to the receiver prior to GFDM data block. The corresponding received signal is expressed as

$$y_{PN} = \boldsymbol{H}_{PN}\boldsymbol{x}_{PN} + \boldsymbol{N}, \tag{9}$$

In timing synchronization, the local sequence generator at the receiver produces a PN sequence of length K to execute the correlation operation with the received y_{PN}. A sliding window w_1 of length K slides point by point, and then the cross-correlation coefficient between the corresponding part of w_1 and the local PN sequence is calculated as

$$R_{PN}(n) = \sum_{i=n}^{n+K-1}\sum_{j=0}^{K-1} y_1(i)x_{PN}(j), \tag{10}$$

Where x_{PN} is the local PN sequence. The correlation coefficient curves of PN-based synchronization when STO values are 0 and ± 10 samples are shown in Fig. 9.

When N_{CP} = 128, the moving distance of the sliding window is only 128 samples. Compared with Fig. 7, there is a distinct single peak for each STO value ($STO = -10$, 0 and 10, respectively), as shown in Fig. 9. It also confirms the good correlation of PN sequence. Therefore, the value of n_{PN} can be determined by detecting the peak of the correlation coefficient. The STO detection result is expressed as

$$n_{PN} = \arg\max\ R_s(n), \tag{11}$$

However, the obtained STO cannot be directly used for synchronization because it is necessary to judge whether the STO is leading to or lagging behind the standard point. In Fig. 9, there are 128 subcarriers in GFDM system. When STO = -10, n_{PN} = 10. When STO = 10, n_{PN} = 118. In the extreme case of large STO, for example, STO = 118, n_{PN} is also equal to 10. Therefore, the further calculation is necessary to determine the actual case of leading or lagging.

Since the preamble consists of two identical PN sequences, the cross-correlation efficient between x_{PN} and the corresponding part of w_1 in Fig. 10 can be calculated to obtain the correlation coefficient expressed as

$$R'_{PN} = \sum_{i=0}^{K-1} y_{PN}(i + n_{PN} + K)x_{PN}(i), \tag{12}$$

For the lagging case as shown in Fig. 10(a), the corresponding position of $n_{PN} + K$ is exactly the beginning of y_2. Because y_2 is identical to y_1, x_{PN} is correlated to y_2 that results in the high cross-correlation coefficient R'_{PN}. Therefore, the lagging case can be determined by the high R'_{PN} and n_{PN} is the actual STO value. Similarly, for the leading case as shown in Fig. 10(b), the corresponding position of $n_{PN}+K$ is not the beginning of y_2 that results in the low cross-correlation coefficient R'_{PN}. Thus, the leading case can be determined by the low R'_{PN} and the actual STO value is $K - n_{PN}$.

After the actual n_{PN} obtained, the STO of GFDM data part can be corrected by zero padding. But in the case of leading, after zero padded to the end of GFDM data and CP removal, the last sub-symbol may suffer from data loss. Here, we use Cyclic Suffix (CS) to eliminate the impact of data loss and maintain the integrity of data after the removals of CP and CS.

In frequency synchronization, the receiver receives two identical PN sequences y_1 and y_2, whose relationship is shown as

$$Y_2(k) = Y_1(k)e^{j2\pi\varepsilon}, \tag{13}$$

Using the relationship of (13), the detected CFO $\hat{\varepsilon}$ can be obtained as

$$\hat{\varepsilon} = \frac{1}{2\pi}\arctan\frac{\sum_{i=0}^{K-1} Re[Y_1^*(i)Y_2(i)]}{\sum_{i=0}^{K-1} Im[Y_1^*(i)Y_2(i)]} \tag{14}$$

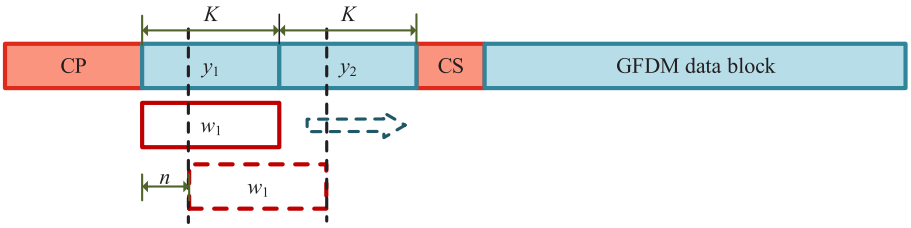

FIGURE 8. PN-based Synchronization.

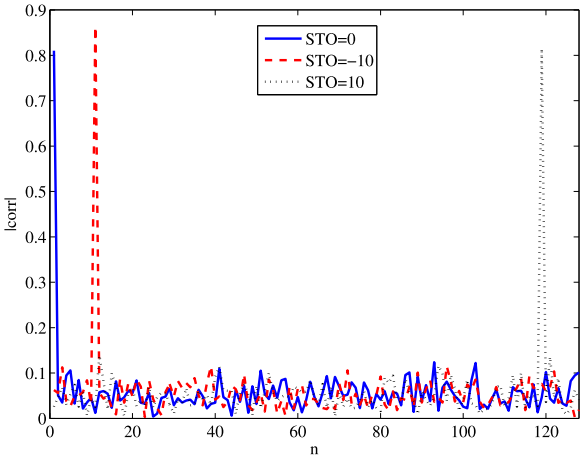

FIGURE 9. Correlation coefficient curves of PN-based synchronization.

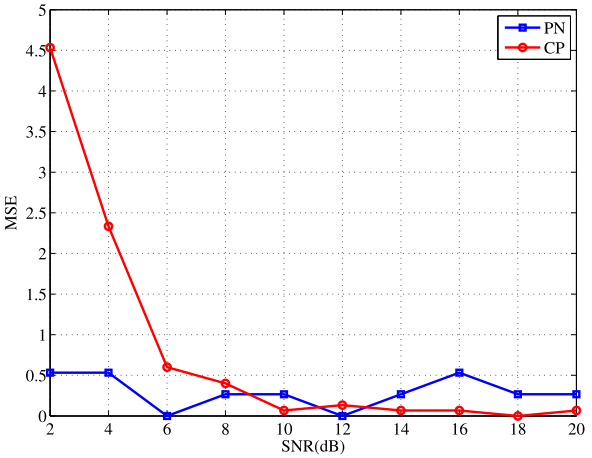

FIGURE 11. MSE comparison of STO synchronization based on CP and PN.

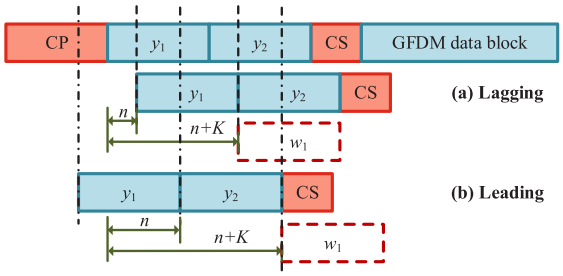

FIGURE 10. Actual STO detection model.

The Mean Square Error (MSE) of $\hat{\varepsilon}$ can be calculated to determine the deviation between $\hat{\varepsilon}$ and the actual CFO as follows

$$MSE_{CFO} = \frac{\sum_{i=0}^{N-1}[\hat{\varepsilon}(i) - \varepsilon]^2}{N}, \tag{15}$$

Where N represents the detection time on the premise of fixed SNR. Since the CFO difference between y_1 and y_2 is ε, the detection range is $(-\pi, \pi)$.

V. SIMULATION RESULTS AND ANALYSIS

In this section, the two approaches in Section III and Section IV are implemented by MATLAB simulations [14]–[17]. The simulation parameters are given as follows. The digital baseband modulation is 16QAM. We set $M = 5$, $K = 128$, $n_{CP} = 128$, the length of CS is $n_{CS} = 64$ and the roll-off coefficient of pulse shaping function $\alpha = 0.2$. The frequency selective channel is used and the multipath number is 2.

As mentioned in Section IV, for timing synchronization, the PN-based synchronization has acute peak of cross-correlation efficient. Besides, for frequency synchronization, if sub-symbol number M is large, the CFO detection range for CP-based synchronization will be reduced, while the PN-based synchronization can maintain the detection range stable. The MSE curves for these two synchronization approaches are shown in Fig. 11 and Fig. 12, respectively.

As shown in Fig. 11, the STO error is large in the case of low SNR for the CP-based synchronization. In contrast, the PN-based synchronization has small STO error and keeps stable MSE for both low and high SNR because of the good correlation of PN sequence.

Fig. 12(a) shows the MSE curves in the case of $M = 5$ and $\varepsilon = 0.05$. In this case, $M\varepsilon = 0.25 < 0.5$, phase flip does not happen to the CP-based synchronization. Both approaches have satisfactory performance at high SNR. Fig. 12(b) demonstrates the MSE curves in the case of $M = 5$ and $\varepsilon = 0.14$. In this case, $M\varepsilon = 0.7 > 0.5$, phase flip happens to the CP-based synchronization leading to that the detected CFO cannot be used directly for synchronization. It can be seen from Fig. 12(b) that the MSE of PN-based synchronization is low and descending.

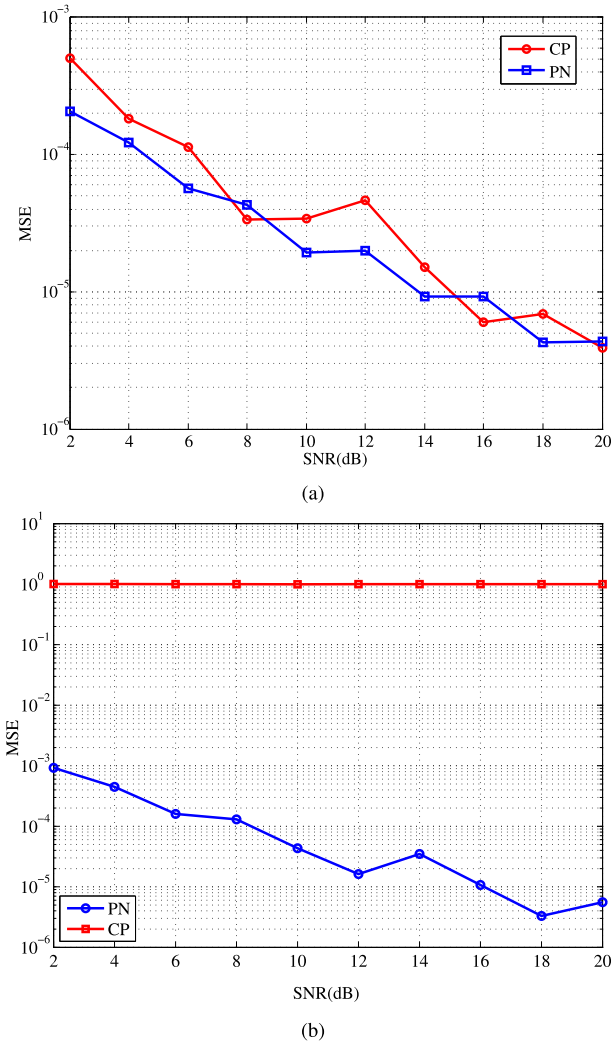

FIGURE 12. MSE comparison of STO synchronization based on CP and PN. (a) $\varepsilon = 0.05$. (b) $\varepsilon = 0.14$.

Therefore, in GFDM system, when the detected ε is in the range of $(-0.5, 0.5)$, the PN-based synchronization has the advantages of stability and simplicity. Although a phase flip occurs when ε is larger than 0.5, the detection range can be expanded by training symbols with multiple repetitive patterns, e.g. we can send a specific period of preamble for CFO estimation, which contains only training sequence without data.

Next, we set $STO = 10$ and the normalized CFO $\varepsilon = 0.15$. Since the complex coding process is not involved in the simulation, SER is selected as the metric to compare the performances of CP-based and PN-based synchronizations. The SER curves are demonstrated in Fig. 13.

In Fig. 13, ZF0 stands for the SER curve without CFO, ZFPN and ZFCP represent the SER curves with $\varepsilon = 0.15$ for the PN-based and CP-based synchronizations, respectively. Compared with the CP-based synchronization, the SER performance for PN-based synchronization is better in the case

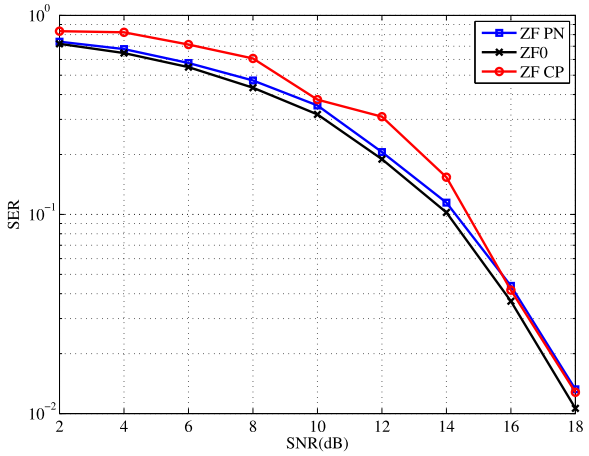

FIGURE 13. SER comparison of CP-based and PN based synchronization.

of a large number of sub-symbols. Even at low SNR, the PN-based synchronization is suitable for GFDM system owing to the reliable offset detection.

VI. CONCLUSION

In this paper, a PN-based synchronization approach for GFDM communication system is proposed. According to the theoretic analysis and simulation results, the following conclusions can be drawn. First, for STO synchronization, the correlation of CP is worse than PN sequence. In this case, the error of correlation detection may lead to high SER. Second, for CFO synchronization, since GFDM data block consists of multiple sub-symbols, the large CFO is prone to phase flip. As a result, the CFO detection range is certainly shrunken. In contrast, the CFO detection range for PN-based synchronization is expended to (-0.5,0.5) and the synchronization complexity is reduced. Although the PN sequence based synchronization may occupy a little more bandwidth than the CP-based synchronization, the approach based on PN sequence can be a qualified candidate for GFDM synchronization if the reliable data transmission is the primary consideration.

ACKNOWLEDGMENT

Declaration of Conflict of Interest: The authors declare that they have no competing interests.

REFERENCES

[1] G. Wunder *et al.*, "5GNOW: Non-orthogonal, asynchronous waveforms for future mobile applications," *IEEE Commun. Mag.*, vol. 52, no. 2, pp. 97–105, Feb. 2014.
[2] M. Jia, Z. Yin, Q. Guo, G. Liu, and X. Gu, "Waveform design of zero head DFT spread spectral efficient frequency division multiplexing," *IEEE Access*, vol. 5, pp. 16944–16952, 2017.
[3] I. S. Gaspar, L. L. Mendes, N. Michailow, and G. Fettweis, "A synchronization technique for generalized frequency division multiplexing," *EURASIP J. Adv. Signal Process.*, vol. 2014, no. 1, pp. 67–76, Dec. 2014. [Online]. Available: http://dx.doi.org/10.1186/1687-6180-2014-67
[4] N. Michailow *et al.*, "Generalized frequency division multiplexing for 5th generation cellular networks," *IEEE Trans. Commun.*, vol. 62, no. 9, pp. 3045–3061, Sep. 2014.

[5] X. Liu, F. Li, and Z. Na, "Optimal resource allocation in simultaneous cooperative spectrum sensing and energy harvesting for multichannel cognitive radio," *IEEE Access*, vol. 5, pp. 3801–3812, 2017.
[6] P. S. Wang and D. W. Lin, "On maximum-likelihood blind synchronization over WSSUS channels for OFDM systems," *IEEE Trans. Signal Process.*, vol. 63, no. 19, pp. 5045–5059, Oct. 2015.
[7] F. Tufvesson, O. Edfors, and M. Faulkner, "Time and frequency synchronization for OFDM using PN-sequence preambles," in *Proc. IEEE Veh. Technol. Conf.*, vol. 4. Sep. 1999, pp. 2203–2207.
[8] X. Liu, J. Liu, H. Sun, H. Liu, and X. Gu, "A timing synchronization method for OFDM based power line communication," in *Proc. IEEE 9th Int. Conf. Commun. Softw. Netw. (ICCSN)*, May 2017, pp. 543–547.
[9] D. Gaspar, L. Mendes, and T. Pimenta, "GFDM BER under synchronization errors," *IEEE Commun. Lett.*, vol. 21, no. 8, pp. 1743–1746, Aug. 2017.
[10] J.-H. Choi, B.-J. Lim, Y.-J. Kim, and Y.-C. Ko, "Effect of timing and frequency synchronization errors on GFDM systems," in *Proc. Int. Conf. Inf. Commun. Technol. Converg. (ICTC)*, Oct. 2015, pp. 1322–1325.
[11] I. Gaspar and G. Fettweis, "An embedded midamble synchronization approach for generalized frequency division multiplexing," in *Proc. IEEE Global Commun. Conf. (GLOBECOM)*, Dec. 2015, pp. 1–5.
[12] T. Kadur, I. Gaspar, N. Michailow, and G. Fettweis, "Non-data aided frequency synchronization exploiting ICI in non-orthogonal systems," in *Proc. IEEE 80th Veh. Technol. Conf. (VTC-Fall)*, Sep. 2014, pp. 1–5.
[13] G. Fettweis, M. Krondorf, and S. Bittner, "GFDM—Generalized frequency division multiplexing," in *Proc. IEEE 69th Veh. Technol. Conf. (VTC Spring)*, Apr. 2009, pp. 1–4.
[14] L. Fan, R. Zhao, F.-K. Gong, N. Yang, and G. K. Karagiannidis, "Secure multiple amplify-and-forward relaying over correlated fading channels," *IEEE Trans. Commun.*, vol. 65, no. 7, pp. 2811–2820, Jul. 2017.
[15] L. Fan, X. Lei, N. Yang, T. Q. Duong, and G. K. Karagiannidis, "Secure multiple amplify-and-forward relaying with cochannel interference," *IEEE J. Sel. Topics Signal Procsess.*, vol. 10, no. 8, pp. 1494–1505, Dec. 2016.
[16] G. Pan *et al.*, "On secrecy performance of MISO SWIPT systems with TAS and imperfect CSI," *IEEE Trans. Commun.*, vol. 64, no. 9, pp. 3831–3843, Sep. 2016.
[17] L. Fan, X. Lei, N. Yang, T. Q. Duong, and G. K. Karagiannidis, "Secrecy cooperative networks with outdated relay selection over correlated fading channels," *IEEE Trans. Veh. Technol.*, vol. 66, no. 8, pp. 7599–7603, Aug. 2017.

ZHENYU NA received the B.S. and M.S. degrees in communication engineering from the Harbin Institute of Technology, China, in 2004 and 2007, respectively, and the Ph.D. degree in information and communication engineering from the Communication Research Center, Harbin Institute of Technology, in 2010. He is currently an Associate Professor with the School of Information Science and Technology, Dalian Maritime University, China. His research interests include satellite communications and networking, OFDM, non-orthogonal multicarrier transmissions, NOMA, and wireless powered communication networks.

MENGSHU ZHANG received the B.S. degree in communication engineering from Dalian Maritime University, Dalian, China, in 2017, where she is currently pursuing the M.S. degree with the School of Information Science and Technology. Her research interests include 5G wireless communications, synchronization, OFDM, NOMA, and satellite communication.

MUDI XIONG received the M.Sc. degree in physics electronics from the Changchun Institute of Optics and Fine Mechanics in 1994 and the Ph.D. degree in optical engineering from the Changchun Institute of Optics, Fine Mechanics and Physics, Chinese Academy of Sciences in 2000. Before 2003, he was an Associate Professor with the Harbin Institute of Technology. In 2003, he came to Dalian Maritime University. Since 2006, he has been the full-time Professor. His research field includes optical signal detection, optical communications, and networking.

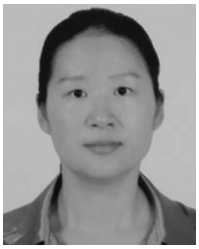

JUNJUAN XIA received the bachelor's degree from the Department of Computer Science from Tianjin University in 2003 and the master's degree from the Department of Electronic Engineering, Shantou University, in 2015. She is currently with the School of Computer Science and Educational Software, Guangzhou University, as a Laboratory Engineer. Her current research interests include wireless caching, physical-layer security, cooperative relaying, and interference modeling.

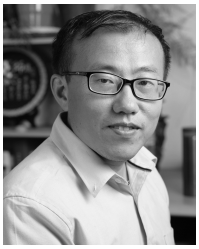

XIN LIU received the M.Sc. and Ph.D. degrees in communication engineering from the Harbin Institute of Technology, in 2008 and 2012, respectively. From 2012 to 2013, he was a Research Fellow with the School of Electrical and Electronic Engineering, Nanyang Technological University, Singapore. From 2013 to 2016, he was a Lecturer with the College of Astronautics, Nanjing University of Aeronautics and Astronautics, China. He is currently an Associate Professor with the School of Information and Communication Engineering, Dalian University of Technology, China. His research interests focus on communication signal processing, cognitive radio, spectrum resource allocation, and broadband satellite communications.

WEIDANG LU (S'08–M'13) received the Ph.D. degree in information and communication engineering from the Harbin Institute of Technology in 2012. He was a Visiting Scholar with Nanyang Technology University, Singapore, also with The Chinese University of Hong Kong, Hong Kong, and also with the Southern University of Science and Technology, China. He is currently an Associate Professor with the College of Information Engineering, Zhejiang University of Technology, Hangzhou, China. His current research interests include simultaneous wireless information and power transfer, wireless sensor networks, cooperative communications, and physical layer security for wireless systems.